Chemical Engineering Journal 161 (2010) 182–190

Contents lists available at ScienceDirect

Chemical Engineering Journal

journal homepage: www.elsevier.com/locate/cej

Modeling adsorption of CO_2 on amine-functionalized mesoporous silica. 2: Kinetics and breakthrough curves

Rodrigo Serna-Guerrero, Abdelhamid Sayari*

Department of Chemical and Biological Engineering, University of Ottawa, 161 Louis Pasteur, Ottawa, ON K1N 6N5, Canada

ARTICLE INFO

Article history:
Received 22 February 2010
Received in revised form 21 April 2010
Accepted 22 April 2010

Keywords:
CO_2 adsorption
MCM-41
Aminosilane grafting
Adsorption kinetics
Adsorption modeling

ABSTRACT

The adsorption kinetics of CO_2 on amine-functionalized mesoporous silica at low concentrations was investigated. Experimental data of CO_2 uptake as a function of time at temperatures between 25 and 70 °C were fit to a series of kinetic models, namely Lagergen's pseudo-first and pseudo-second order and Avrami's kinetic models. The best fit was obtained using Avrami's model, as it provided a fractional reaction order (ca. 1.4), which has been associated with the occurrence of multiple adsorption pathways. In addition, simulations of CO_2 adsorption in a column packed with amine-grafted mesoporous silica using computational fluid dynamics were carried out to predict breakthrough curves. The simulation results were compared to experimental data produced at various flow rates of a stream containing 5% CO_2 balance nitrogen. In all cases, the predicted breakthrough time and the corresponding CO_2 uptake were in close agreement with the experimental data.

1. Introduction

The deleterious effects of greenhouse gases on the environment and the threat they pose on the sustainability of ecosystems have fuelled the search for novel technologies capable of minimizing their emissions into the atmosphere. In particular, being the main anthropogenic contributor to climate change, carbon dioxide (CO_2) emissions have prompted a wide range of corrective initiatives to mitigate their impact. In addition to CO_2 capture to address environmental concerns, the removal of CO_2 in gas streams is required in other applications including air purification in confined spaces [1,2] and natural gas treatment, among others [3,4]. Consequently, researchers are actively exploring more efficient CO_2 capture technologies [5,6].

Among the alternatives currently investigated for CO_2 capture, adsorption separation technologies have drawn particular attention since they can produce high purity streams with low energy consumption. As a result, a wide variety of adsorbents have been studied in recent years for such purpose [7]. As reported elsewhere [8,9], our research group developed a promising CO_2 adsorbent, referred to as TRI-PE-MCM-41, which consists of triamine-bearing organic species grafted on a mesoporous MCM-41 silica, whose pores were enlarged by post-synthesis hydrothermal treatment. This material was engineered to accommodate high loadings of amine functional groups while minimizing diffusion limitations. Indeed, TRI-PE-MCM-41 exhibited high adsorption capacity with an unprecedentedly fast rate of adsorption compared to other amine-functionalized adsorbents reported in literature [8]. Furthermore, unlike typical commercial adsorbents such as zeolites, TRI-PE-MCM-41 is tolerant to moisture in the feed and is highly selective towards acid gases in mixtures with nitrogen, oxygen, hydrogen and methane even at very low concentrations [9–11]. In addition, it was demonstrated in a recent contribution that TRI-PE-MCM-41 is stable over a series of adsorption–desorption cycles when appropriate regeneration conditions (e.g., 70 °C under vacuum) are used [11]. Because of the excellent attributes offered by amine-functionalized CO_2 adsorbents in general, and TRI-PE-MCM-41 in particular, it is interesting to model their adsorption characteristics to gain a better understanding of their behavior and for the simulation of CO_2 capture processes using such materials.

In a separate contribution, an adsorption equilibrium model for CO_2 on amine-functionalized silicas was developed based on the occurrence of two independent adsorption mechanisms [12]. The development of this model stems from earlier observations regarding the interactions of CO_2 with amine-grafted mesoporous silica under dry and humid conditions [13]. The data indicated that in the presence of dry gaseous feed, CO_2 interacts chemically with amine groups with a maximum CO_2/N ratio of 0.5, consistent with the formation of carbamate species, an observation that has been corroborated by other groups using infrared spectroscopy [14,15]. In addition, CO_2 can also adsorb physically on the surface of the material, particularly at pressures beyond 0.05 bar at room temperature. The equilibrium model was capable of describing the adsorption of CO_2 and H_2S over a wide range of concentrations and tempera-

* Corresponding author.
E-mail address: abdel.sayari@uottawa.ca (A. Sayari).

1385-8947/$ – see front matter © 2010 Elsevier B.V. All rights reserved.
doi:10.1016/j.cej.2010.04.042

Table 1
Kinetic adsorption models.

Kinetic model	Equation	Differential form
Pseudo-first order	$q_t = q_e[1-\exp(-k_f t)]$	$\frac{dq_t}{dt} = k_f(q_e - q_t)$
Pseudo-second order	$q_t = \frac{k_s q_e^2 t}{1+q_e k_s t}$	$\frac{dq_t}{dt} = k_s(q_e - q_t)^2$
Avrami	$q_t = q_e[1-\exp(-(k_A t)^{n_A})]$	$\frac{dq_t}{dt} = k_A^n t^{n-1}(q_e - q_t)$

ture on our material and others, while providing parameters for the prediction of adsorption capacity at equilibrium, based on the structural properties of the adsorbent and its amine loading.

To gain further insights into the CO_2 adsorption on amine-functionalized adsorbents and with the aim of building a strong basis for simulation, the current contribution was devoted to the development of a suitable kinetic model. To the best of our knowledge, no kinetic models for CO_2 adsorption on amine-functionalized mesoporous silica have been proposed so far. In addition, based on the proposed kinetic model and the equilibrium model developed in a separate contribution [12], we were able to simulate the adsorption of CO_2 in a fixed bed column using computational fluid dynamics.

1.1. Kinetic models

Among the properties expected in a good adsorbent, fast adsorption kinetics is one of the most important, since the efficiency of an adsorbent in dynamic processes, e.g., adsorption in a fixed bed column, and its capacity to withstand large adsorbate flows are associated with its rate of adsorption. Currently, the literature provides a wide number of kinetic models. Because of the complexity involved in the prediction of kinetic parameters, a typical approach consists of fitting experimental data to a series of established models, and selecting the one that provides the best fit. In recent years, however, several researchers attempted to rationalize some of the most popular kinetic models [16–18], making it possible to deduce information regarding the adsorbent–adsorbate interactions. Three such models will be considered in this work, including two of the most widely applied kinetic models, namely, Lagergen's pseudo-first order and pseudo-second order kinetic models [19]. A fractional order kinetic model was recently developed based on Avrami's kinetic model of particle nucleation [20] and was applied to describe the adsorption of anionic dyes on an aminopropyl-functionalized silica [21], making it attractive for our work. Table 1 shows the list of equations associated with the kinetic models explored in this work, where t is the time elapsed from the beginning of the adsorption process, q_t is the amount adsorbed at a given point in time, and q_e represents the amount adsorbed at equilibrium.

To determine the adequacy of each model, an error function based on the normalized standard deviation (Eq. (1)) was applied:

$$\mathrm{Err}(\%) = \sqrt{\frac{\sum[(q_{t(\exp)} - q_{t(\mathrm{mod})})/q_{t(\exp)}]^2}{N-1}} \times 100 \quad (1)$$

where Err(%) is the error function, $q_{t(\exp)}$ is the amount adsorbed at a given time determined experimentally, $q_{t(\mathrm{mod})}$ is the amount adsorbed as predicted by the model and N is the total number of experimental points.

Accordingly, it is necessary to determine q_e to completely define a kinetic model. As mentioned earlier, we developed an equilibrium model to describe the adsorption over a wide range of CO_2 pressure at temperatures from 25 to 55 °C [12]. Although CO_2 adsorption isotherms on TRI-PE-MCM-41 have already been reported, a typical adsorption isotherm for CO_2 on TRI-PE-MCM-41 is shown in Fig. 1 for illustration. In addition, the model used to fit this data is expressed in Eq. (2):

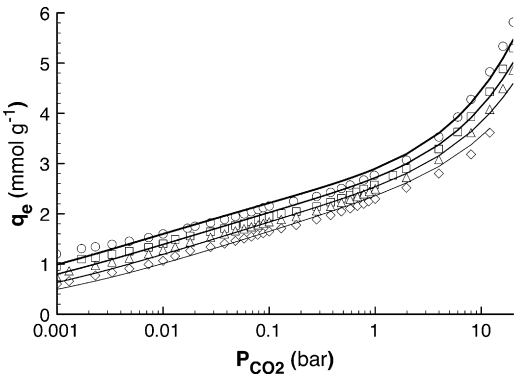

Fig. 1. CO_2 adsorption isotherm on TRI-PE-MCM-41 at 25 °C (circles), 35 °C (squares), 45 °C (triangles) and 55 °C (diamonds). The solid lines represent the isotherm model fit.

$$q_e = \left[\frac{n_s b P}{(1+(bP)^t)^{1/t}}\right]_{chem} + \left[\frac{n_s b P}{(1+(bP)^t)^{1/t}}\right]_{phys} \quad (2)$$

where n_s, b and t are the characteristic parameters of the model and the subscripts "*chem*" and "*phys*" denote the contribution of chemical and physical adsorption, respectively.

The temperature-dependent forms of the model coefficients are:

$$b = b_0 \exp\left[\frac{\Delta H}{RT_0}\left(\frac{T_0}{T} - 1\right)\right]$$

$$t = t_0 + \alpha\left(1 - \frac{T_0}{T}\right)$$

$$n_s = n_{s0} \exp\left[\chi\left(1 - \frac{T}{T_0}\right)\right]$$

where ΔH is the heat of adsorption at loadings close to zero, R is the universal ideal gas constant, α and χ are the parameters of the temperature-dependent form of the Toth model and the subscript 0 refers to the parameters obtained at a reference temperature T_0. The values of the equilibrium model parameters for CO_2 adsorption using 25 °C as reference temperature are presented in Table 2.

1.2. Fixed bed column modeling

The establishment of equilibrium and kinetic models contributes to the understanding of the adsorption phenomena, but one of their main objectives from an engineering standpoint is the description of a process for simulation and modeling. Using appropriate equilibrium and kinetic equations, the behavior of a fixed bed column can be predicted. By comparison with experimental data, it is possible to validate the adequacy of the model proposed.

Table 2
Isotherm parameters for CO_2 adsorption on TRI-PE-MCM-41 using 25 °C as reference temperature.

CO_2 uptake	n_{s0} (mmol g^{-1})	b_0 (bar^{-1})	t_0	χ	α	ΔH (kJ mol^{-1})
q_{phys}	6.98	2.74×10^{-1}	9.62×10^{-1}	5.35	0	19.2
q_{chem}	3.64	1.25×10^{5}	2.24×10^{-1}	0	6.05×10^{-2}	67.3

For adsorption in a fixed bed column, the mass transfer in the gas phase can be modeled as a dispersed plug flow accounting for mixing in the axial direction. As a general rule, the difference of concentration in the radial direction is considered negligible when the ratio of the column-to-particle radius is sufficiently large, typically above 10. The general mass balance equation for an adsorption packed bed column is:

$$\varepsilon\left[D_L\frac{\partial^2 C_A}{\partial z^2}\right]-u_s\frac{\partial C_A}{\partial z}-(1-\varepsilon)\left[\rho_p\left(\frac{dq}{dt}\right)\right]=\varepsilon\frac{\partial C_A}{\partial t} \quad (3)$$

where D_L is the axial dispersion of the adsorbate in the gas stream, z is the length in the axial direction, u_s is the superficial velocity of the gas mixture, ε is the bed void fraction, t is time, C_A is the concentration of the adsorbate in the gas phase and (dq/dt) is the rate of adsorption. In the present study, the term (dq/dt) was calculated from the kinetic models described in Section 1.1. The coefficients of the various kinetic models are lumped values representing the various levels of gas phase diffusion onto the solid adsorbent until equilibration between the gas and adsorbed phases.

To solve the mass balance equation, the following assumptions and limits were used:

At $t<0: C_A=0; \quad q=0$

At $t>0: C_{A@z=0}=C_0; \quad (dC_A/dz)_{@z=L}=(dC_A/dz)_{@z=L-dz}$

At $t=\infty: C_A=C_0$

where C_0 is the concentration of the feed.

In this work, the inlet concentration of CO_2 was set at 5% balance nitrogen since this concentration is of interest for some potential applications, e.g., flue gas treatment and air purification in closed-circuit breathing systems. It is thus possible to consider the gas stream as a dilute solution, a condition under which the fluid velocity across the bed length is deemed constant. In addition, because of the low concentration of CO_2, an isothermal column operation was assumed. This assumption simplifies the model since the mass balance can be described without the use of an energy balance. While admittedly the operation of a real adsorption column is typically adiabatic, it should be mentioned that the experiments were performed in a column located inside a temperature-controlled enclosure, which might lend support to the approximation of isothermal conditions for this first attempt at modeling CO_2 adsorption on amine-grafted mesoporous silica.

The mass balance equation was solved by computational fluid dynamics using the finite volume method [22]. This method permits the solution of partial differential equations by the discretization of the system into segments referred to as control volumes. It is assumed that concentration varies linearly within the limits of the control volume and the mass transfer at the limits of each control volume is continuous. The result is a series of simultaneous equations from which it is possible to calculate the concentration throughout discrete points of space and time. The accuracy of this method relies heavily on the size of control volumes, with smaller sizes providing a more accurate description of the system but with increased computational requirements. In this work, the convective–dispersive mass transfer was modeled using the hybrid scheme in which the influence of axial dispersion is considered significant only at Peclet numbers lower than 2. The transient state was approximated with the totally implicit scheme, in which the change of adsorbate concentration in each control volume as a function of time is considered to be dependent only on the conditions of the previous step in time. An iterative solution routine was programmed using Microsoft Excel® Visual Basic for Applications.

2. Experimental

2.1. Materials

Cab-O-Sil M-5 fumed silica from Cabot was used as the silica source. Cetyltrimethylammonium bromide (CTAB, Aldrich) and tetramethylammonium hydroxide (TMAOH 25%, balance water, Aldrich) were used as structure directing agent and for pH adjustment, respectively. The post-synthesis pore expander agent was dimethyldecylamine (DMDA 97% purity, Aldrich). The grafting agent 2-[2-(3-trimethoxysilylpropylamino)ethylamino]ethylamine (herein referred to as TRI-silane) and polyethyleneimine (PEI, M_n = 423) were obtained from Sigma–Aldrich. Ultra high purity grade nitrogen and certified gas mixture of 5% CO_2 balance N_2 were supplied by Linde Ltd., Canada. All reagents and gases were used without further purification.

2.2. Synthesis of adsorbent

Detailed description of the synthesis of the amine-functionalized mesoporous material used in the present work was reported by Harlick and Sayari [8]. Briefly, MCM-41 type silica was produced at 100 °C in the presence of CTAB in basic conditions using TMAOH. Subsequently, the pore size of MCM-41 was increased by hydrothermal restructuring at 120 °C in the presence of DMDA [23]. The surfactant template and pore expander agent were removed by calcination in nitrogen, then in air at 550 °C, and the resulting material was labeled PE-MCM-41. The amine functional groups were incorporated onto PE-MCM-41 by grafting in toluene at 85 °C in a 250 mL glass reactor. First, 0.3 mL of water per g of silica was added to a PE-MCM-41 silica suspension in toluene, followed by addition of TRI-silane (3 mL per g of silica). Grafting proceeded for 16 h, and then the product was filtered and washed with toluene and pentane. The solid obtained was dried in a natural convection oven at 100 °C for 1 h and labeled TRI-PE-MCM-41. Finally, as fine powder produces large pressure drops in packed bed columns, pellets were produced as follows. The powdered form of TRI-PE-MCM-41 was loaded in a dye and compressed under a load of 450 kg cm^{-2} using a hydraulic press. As reported earlier, such a pressure did not affect significantly the structural properties of the adsorbent [24]. The particles thus produced were crushed and sieved between openings of 0.82 and 0.41 mm (i.e., 20 and 40 mesh, respectively). Another sample used in this investigation was prepared by dispersing PEI on PE-MCM-41, following the recipe by Xu et al. [25]. An amount of 1 g of PEI was dispersed in methanol at room temperature followed by addition of 1 g PE-MCM-41 to the mixture under continuous stirring. The mixture was stirred overnight under ambient air until complete evaporation of the solvent. The resulting solid was labeled as PEI-PE-MCM-41.

2.3. Characterization

The structural properties of the adsorbent were determined by nitrogen adsorption measurements at 77 K using a Micromeritics ASAP 2020 volumetric instrument. The sample was treated under vacuum (i.e., 0.5 mmHg) at 100 °C for 5 h before adsorption measurements. Surface area was determined using the BET method, while the pore volume was considered as the volume of liquid nitrogen adsorbed at a relative pressure close to 1. The pore size distribution was obtained using the KJS method [26]. Additionally, the organic content was determined by thermogravimetric analysis (TGA) using a TA Q-500 instrument. The sample was heated at 10 °C min^{-1} under flowing nitrogen up to 800 °C followed by decomposition in the presence of air at the same heating rate and up to 1000 °C.

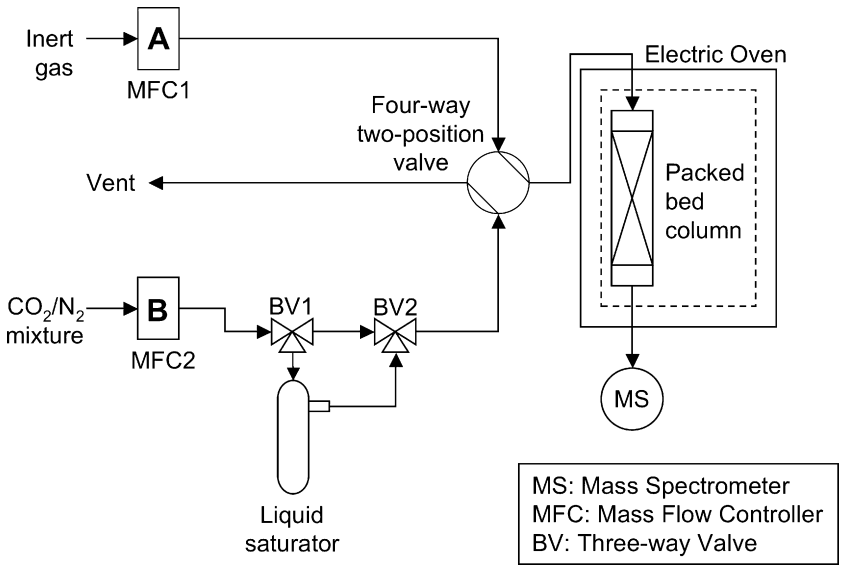

Fig. 2. Experimental setup for CO_2 adsorption in a packed bed column.

2.4. CO_2 adsorption measurements

The uptake of CO_2 as a function of time was monitored using the TA instrument mentioned above. A sample of ca. 0.03 g of TRI-PE-MCM-41 was loaded in a platinum crucible with a depth of 5 mm. Once loaded, the sample was activated by heating at 10 °C min^{-1} up to 150 °C for TRI-PE-MCM-41 and up to 100 °C for PEI-PE-MCM-41 under flowing nitrogen for 2 h. It was then cooled to the desired temperature (i.e., 25, 40, 55 or 70 °C) and exposed to a flowing mixture of 5% CO_2 balance nitrogen at 100 mL min^{-1}. Previous studies showed that under such conditions, adsorption of nitrogen on TRI-PE-MCM-41 is negligible [9]. According to the analysis presented by Barrie et al. [27], for gravimetric measurements in a microbalance, when a shallow layer of adsorbent is combined with a sufficiently high adsorbate flow rate, the influence of axial dispersion through the adsorbent layer does not affect significantly the experimental measurement. Furthermore, similarly to zero-length columns, it was proven that at low adsorbate concentration the operation could be considered isothermal despite the inherent release of heat associated with CO_2 adsorption. Since our experimental procedure meets these conditions, the assumptions of negligible axial dispersion and isothermal operation were considered adequate for the TGA measurements. The experimental CO_2 uptake as a function of time was fitted to each kinetic model listed in Table 1 using a regression on their linearized forms.

The experimental setup used for CO_2 adsorption studies in a packed bed column is represented schematically in Fig. 2. A sample of ca. 0.45 g of TRI-PE-MCM-41 with 20–40 mesh particle size was loaded in a stainless steel column with inner diameter of 0.43 and 12 cm of packed height. Before each run, the adsorbent was activated for 2 h using a flow of 50 mL min^{-1} of helium, while maintaining the column at 150 °C using an electric oven with temperature control. The temperature was then lowered to 25 °C, and the flow was switched to a mixture of 5% CO_2 balance nitrogen at 50, 30 or 15 mL min^{-1}, equivalent to a contact time of 0.024, 0.04 and 0.08 min, respectively. The column downstream was continuously monitored using a Pfeiffer Thermostar mass spectrometer (MS). The experimental breakthrough curves of CO_2 were obtained from the MS signal corresponding to 44 amu.

The dynamic adsorption capacity (q) of the column was calculated using Eq. (4):

$$q = \frac{FC_0 t_q}{W} \tag{4}$$

where F is the total molar flow, C_0 is the concentration of the adsorbate in the feed stream, W is the mass of adsorbent loaded in the column, and t_q is the stoichiometric time, which is estimated from the breakthrough profile according to Eq. (5) [28]:

$$t_q = \int_0^\infty \left(1 - \frac{C_A}{C_0}\right) dt \tag{5}$$

where C_0 and C_A are the concentrations of the adsorbate upstream and downstream the column, respectively.

3. Results and discussion

Nitrogen adsorption–desorption isotherms for TRI-PE-MCM-41 and PE-MCM-41 are presented in Fig. 3, while TGA profiles are shown in Fig. S1 (Supplementary Information). The structural properties deduced from nitrogen adsorption data are presented in Table 3. The shape of the nitrogen adsorption isotherms for PE-MCM-41 and TRI-PE-MCM-41 correspond to Type IV according to the IUPAC classification, which is associated with mesoporous materials. Fig. 3 also shows that after impregnation of PEI on PE-MCM-41, most of its pore volume and surface area were lost, in agreement with observations by other workers studying PEI-

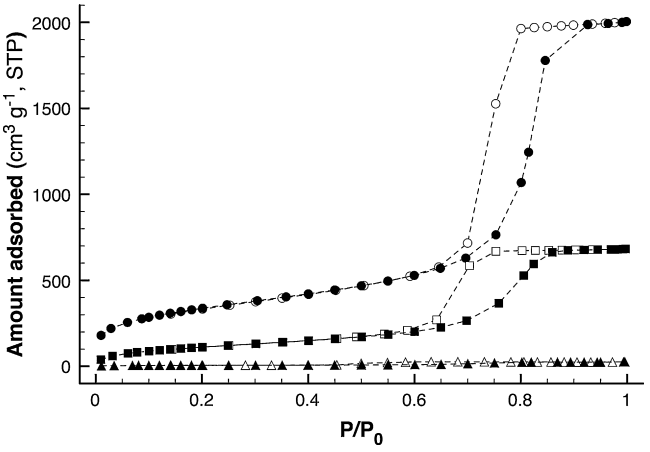

Fig. 3. Nitrogen adsorption (closed symbols) and desorption (open symbols) isotherms for PE-MCM-41 (circles), TRI-PE-MCM-41 (squares) and PEI-PE-MCM-41 (triangles).

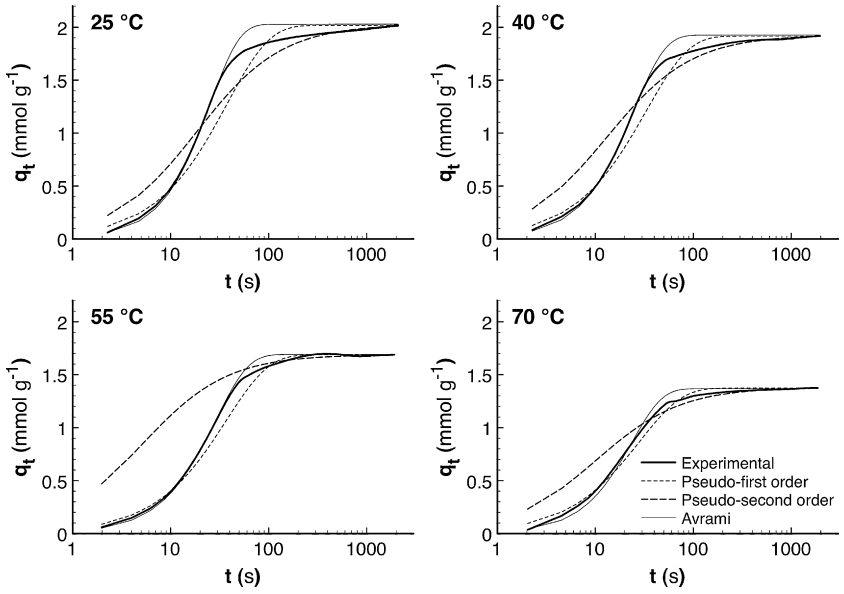

Fig. 4. Experimental CO_2 uptake on TRI-PE-MCM-41 and corresponding fit to kinetic models.

Table 3
Structural properties of mesoporous materials.

	Surface area ($m^2\ g^{-1}$)	Pore volume ($cm^3\ g^{-1}$)	Mean pore size (nm)
PE-MCM-41	1134	2.62	10.9
TRI-PE-MCM-41	429	1.05	9.6
PEI-PE-MCM-41	21	0.04	8.2

loaded mesoporous silica with high organic content [25,29–32]. Moreover, TRI-PE-MCM-41 maintained a mesoporous nature after the incorporation of functional groups, which is a key feature for an effective adsorbent [13]. Although incorporation of organic molecules resulted in a decreased surface area, in the case of TRI-PE-MCM-41 it remained relatively high ($429\ m^2\ g^{-1}$). The loading of amine groups for TRI-PE-MCM-41 was $7.27\ mmol\ g^{-1}$.

3.1. Adsorption kinetics

Fig. 4 shows the CO_2 uptake vs. time at 25, 40, 55 and 70 °C, and the corresponding profiles as predicted by the different kinetic models. In general, fast adsorption kinetics were observed with more than 80% of the total CO_2 uptake on TRI-PE-MCM-41 occurring within the first 40 s of contact time. Table 4 shows the values of the kinetic constants and the characteristic parameters of the kinetic models, along with the associated errors as calculated using Eq. (1).

It was observed that the pseudo-first and pseudo-second order kinetic models presented some limitations with respect to the prediction of CO_2 adsorption on TRI-PE-MCM-41. At 25 °C for example, after a few seconds the pseudo-first order model underestimated the CO_2 uptake, up to ca. 100 s. After this time, the CO_2 adsorbed was consistently overestimated until the process approached equilibrium. On the other hand, the pseudo-second order appeared to fit the process accurately, but only beyond ca. 300 s. These results are in agreement with earlier reports, suggesting that the pseudo-first order kinetic model is applicable only under low surface coverage, and hence describes the early stages of adsorption [18,33]. It was also proposed that the pseudo-second order kinetic model represents adsorption at high adsorbate loadings. The adequacy of the pseudo-first order kinetic model at low surface coverage can be used to describe the behavior of CO_2 adsorption on purely siliceous MCM-41 and PE-MCM-41, for example. Indeed, because of the low adsorption capacity of non-functionalized mesoporous silica at CO_2 concentration of 5%, the surface coverage can be considered low, even at equilibrium. Hence, as previously reported by our group [9], the pseudo-first order kinetics successfully described CO_2 adsorption on purely siliceous adsorbents. However, when applied to CO_2 adsorption on the functionalized adsorbent, this model presented some limitations, deviating significantly from the experimental data after the first few seconds of the adsorption process, presumably after the adsorbate surface coverage became high enough. This is clearly consistent with the plot of the linearized form of the kinetic model, available in Supplementary Data (Figure S2), where a deviation from linearity occurred after a few seconds of contact time. Nonetheless, for practical purposes, the values of k_f presented in Table 4 can be used within an acceptable degree of accuracy, since the calculated error within the range of temperature considered did not exceed 8%. The attractiveness in using the

Table 4
Values of the kinetic model parameters for CO_2 adsorption on TRI-PE-MCM-41.

		25 °C	40 °C	55 °C	70 °C
Pseudo-first	k_f (s^{-1})	3.61×10^{-2}	3.96×10^{-2}	4.01×10^{-2}	4.12×10^{-2}
	Err(%)	5.7	4.5	3.1	8.3
Pseudo-second	k_s ($g\ mmol^{-1}\ s^{-1}$)	2.10×10^{-2}	3.11×10^{-2}	5.06×10^{-2}	5.63×10^{-2}
	q_e ($mmol\ g^{-1}$)	2.06	1.95	1.71	1.40
	Err(%)	12.8	13.0	36.2	27.1
Avrami	k_A (s^{-1})	3.92×10^{-2}	4.02×10^{-2}	4.12×10^{-2}	4.21×10^{-2}
	n_A	1.46	1.36	1.41	1.41
	Err(%)	3.5	2.8	1.7	2.8

Table 5
D_S/r_p^2 (s^{-1}) values for CO_2 adsorption on TRI-PE-MCM-41 and NaY.

	TRI-PE-MCM-41		NaY [36]
	Pseudo-first	Fickian	
25 °C	2.41×10^{-3}	2.66×10^{-3}	3.01×10^{-4}
40 °C	2.64×10^{-3}	2.96×10^{-3}	6.77×10^{-4}
55 °C	2.67×10^{-3}	2.98×10^{-3}	1.41×10^{-3}
70 °C	2.74×10^{-3}	3.06×10^{-3}	2.76×10^{-3}

pseudo-first order kinetic model is twofold: (i) due to its simple mathematic expression, it has been widely applied for the study and modeling of adsorption systems and (ii) it can be used to determine kinetic properties like micropore diffusion when the geometry of the particles is known [34]. For example, if interparticle diffusion is considered the rate-limiting step and the particles are assumed to be comprised of spheres with the same size, a diffusivity factor can be calculated using Eq. (6):

$$k_f = 15\frac{D_S}{{r_p}^2} \tag{6}$$

where D_S is the diffusivity in the solid and r_p is the radius of a particle.

It is also possible to obtain values of diffusivity from the experimental uptake profile using a Fickian diffusion model of the form [35]:

$$\frac{q_t}{q_e} = 1 - \frac{6}{\pi^2}\sum_{n=1}^{\infty}\frac{1}{n^2}\ \exp\left(-n^2\pi^2\frac{D_S}{{r_p}^2}t\right) \tag{7}$$

Accordingly, the Fickian diffusion model was used to corroborate the values of D_S/r_p^2 calculated from the pseudo-first order model (Eq. (6)). A value of D_S/r_p^2 can be obtained from the slope of a linearized form of Eq. (7). A plot of CO_2 uptake on TRI-PE-MCM-41 and its fit to the linearized form of Eq. (7) can be found in Supporting Information, along with its corresponding linear regression parameters (Figure S5 and Table S1). Table 5 shows that the values of D_S/r_p^2 obtained using both approaches are within ca. 10% from each other. The closeness of D_S/r_p^2 values suggests that the first order kinetic model parameters can be used with an acceptable level of confidence to describe the CO_2 uptake on TRI-PE-MCM-41. The difference between these values can be mainly attributed to the assumptions of particle shape and equal size used in Eq. (6), as deviations likely occurred. For comparison, Table 5 also shows values of D_S/r_p^2 reported in literature for CO_2 adsorption on NaY zeolite [36]. The relatively higher values of D_S/r_p^2 in the case of TRI-PE-MCM-41 represent lower diffusion limitations, which can be attributed to a larger pore size than NaY zeolite and could be translated into faster adsorption kinetics.

As seen in Fig. 5, the pseudo-second order kinetic model fits the experimental data once the CO_2 uptake slows down. Although a good fit was obtained on the linearized form of the pseudo-second order model (Supporting Information, Figure S3), the value of Err(%) was higher compared with the pseudo-first order model, the main source of error being its inability to fit the uptake at the beginning of the process. However, other characteristics of the pseudo-second order kinetic model may be useful. For example, this model does not require *a priori* determination of the amount adsorbed at equilibrium, as it can be deduced from the linear regression of the experimental data [19]. The values of q_e reported in Table 4 reflected closely the experimental adsorption capacity at equilibrium. Nevertheless, as observed by Royer et al. [37], the value of k_s depends strongly on the initial concentration of the adsorbate.

The best fit to a kinetic model was obtained using Avrami's equation. The calculated order of this model was of ca. 1.4, and varied in less than 5% with respect to the adsorption temperature

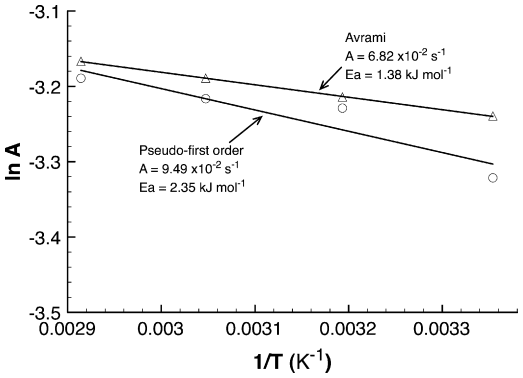

Fig. 5. Arrhenius plots for the kinetic constants obtained by pseudo-first order and Avrami kinetic models.

within the range studied. According to Cestari et al. [20,21], the fractional order of this model stems from the complexity of the reaction mechanisms or the occurrence of more than one reaction pathway. It is thus possible that the excellent fit of Avrami's kinetic model resulted from its capacity to account for the CO_2 uptake by chemical and physical adsorption demonstrated earlier [13]. A further advantage of Avrami's equation is that the kinetic constant, expressed in s^{-1}, is independent of the initial concentration of the adsorbate [37].

Since the pseudo-first order kinetic model and Avrami's model were considered adequate, we used the corresponding kinetic coefficients at various temperatures (i.e., 25, 40, 55 and 70 °C) to calculate the parameters of an Arrhenius type equation (Eq. (8)) by a linear regression on its linearized form:

$$k = A\ \exp\left(\frac{-E_a}{RT}\right) \tag{8}$$

where A is the Arrhenius preexponential factor, E_a is a term associated with the activation energy, R is the universal ideal gas constant, and T is temperature. Eq. (8) can be used to predict values of the kinetic constant (k) at a certain temperature, which can be useful to describe non-isothermal behavior.

Fig. 5 shows the plots of the linearized Arrhenius equation, along with the corresponding values of A and E_a. As seen, there is a discrepancy between the values of E_a for the different kinetic models. However, caution should be exercised when attempting to associate E_a with the actual activation energy in the case of models with a kinetic order other than one. For example, as demonstrated by Azizian et al. [17], the value of k obtained from the pseudo-second order kinetic model is not the kinetic constant for adsorption in a strict sense, but rather a complex function involving different parameters such as the kinetic constant for desorption, the surface coverage at equilibrium and the change of adsorbate concentration during the process. In a similar manner, the fractional order in the Avrami model suggests that the value of k_A is an overall constant representing various reaction steps. The Arrhenius equation in these cases is useful to predict k at different temperatures, although the adequacy of these semi-empirical models to determine thermodynamic parameters is still debatable.

Recent effort was devoted to the development of PEI-impregnated on mesoporous silica [25,29–32] and carbon [38,39] as they reportedly exhibit high CO_2 adsorption capacity. Consequently, it was of interest to determine the kinetic properties of PEI-impregnated PE-MCM-41 silica for comparison with TRI-PE-MCM-41. Fig. 6 shows profiles of CO_2 uptake on PEI-PE-MCM-41 at 25 and 70 °C. According to most of the reports presented in the literature, the optimum CO_2 uptake on PEI-impregnated materials, in terms of both adsorption capacity and kinetics, was observed at ca. 75 °C. However, this was not the case of the present study. While it

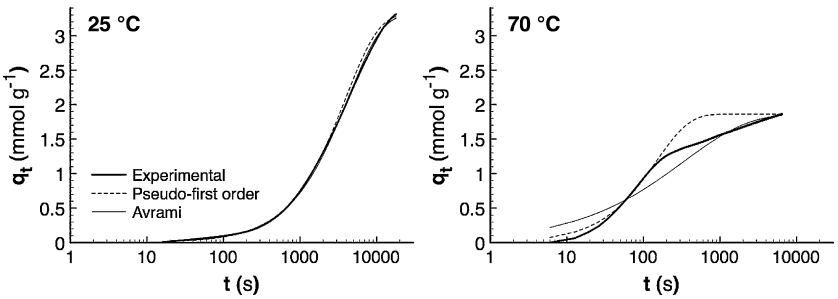

Fig. 6. Experimental CO_2 uptake on PEI-PE-MCM-41 and corresponding fit to kinetic models.

was evident that PEI-PE-MCM-41 presented a slow uptake at room temperature, after a long contact time it exhibited a high q_e. The adsorption capacity was lower at 75 °C, but its kinetic behavior was much more favorable, reaching an uptake of 80% of its total capacity after ca. 10 min of contact time. Thus, it is possible that either (i) the results at room temperature presented in previous studies were not at, or sufficiently close to, equilibrium due to the particularly slow kinetics, producing an apparently higher q_e at ca. 75 °C because of significantly improved kinetics, or (ii) the large pores of the support used in this work offered a comparative advantage permitting a better, albeit slow, access to amine groups even at room temperature. The unfavorable kinetics of PEI-impregnated materials at room temperature has been widely reported [25,29–32], and a series of explanations have been put forth. In general, it is believed that PEI agglomerates in a bulk, liquid-like phase inside the pores, generating strong diffusion limitations to CO_2 leading to an inefficient use of amine groups. As temperature increases, diffusion through the PEI phase improves accompanied with a facilitated uptake of CO_2.

Table 6 shows the kinetic parameters obtained for PEI-PE-MCM-41 using the pseudo-first and Avrami's kinetic models. It was observed that the first order kinetics provided an adequate description of the adsorption of CO_2 at 25 °C since the Err(%) value was small and even Avrami's model produced a kinetic order close to unity. This was not the case at 70 °C, as Avrami's kinetic order was a fractional value, suggesting a change in adsorption mechanisms, consistent with the hypothesis that a different physical state of PEI occurs at higher temperature. It was also evident that even at 70 °C, the kinetics of CO_2 adsorption on PEI-PE-MCM-41 is comparatively slower than that of TRI-PE-MCM-41. Since Avrami's model produced orders with different values, a fair comparison can be made based on k_f for the first order kinetics model. As seen, PEI presented a k_f of 6.81×10^{-3} at 70 °C, while it was 4.12×10^{-2} for TRI-PE-MCM-41 under the same conditions. The comparison was more dramatic for adsorption at room temperature, where TRI-PE-MCM-41 had a kinetic constant two orders of magnitude higher than its PEI-impregnated counterpart. The combination of high amine loading and open pore structure represents a distinct advantage of TRI-PE-MCM-41 in terms of rate of adsorption. It is thus reasonable to conclude that, although a high concentration of amine groups can be obtained by PEI impregnation on mesoporous silica, the favorable kinetics of TRI-PE-MCM-41 leads to more efficient CO_2 separation processes.

Table 6
Values of the kinetic model parameters for CO_2 adsorption on PEI-PE-MCM-41.

		25 °C	70 °C
Pseudo-first	k_f (s^{-1})	2.53×10^{-4}	6.81×10^{-3}
	Err(%)	6.3	12.4
Avrami	k_A (s^{-1})	2.35×10^{-4}	2.96×10^{-3}
	n_A	0.97	0.52
	Err(%)	6.3	17.9

Table 7
Adsorption bed characteristics and operating conditions for fixed bed adsorption experiments.

Packed bed length (z)	12 cm
Inner column diameter	0.42 cm
Bed porosity (ε)	0.38
Particle density (ρ_p)	880 mg cm^{-3}
Feed gas composition	5% CO_2; 95% N_2
Total pressure	1 atm
Axial dispersion coefficient (D_L)	0.167 cm^2 s^{-1} [a]

[a] *Source*: Geankoplis [28].

3.2. Fixed bed column adsorption

To predict breakthrough curves, we studied the adsorption of CO_2 in a fixed bed column packed with TRI-PE-MCM-41 pellets. The characteristics of the adsorption bed and the operating conditions are summarized in Table 7. A series of typical experimental breakthrough curves of CO_2 are presented in Fig. 7. The steep nature of these curves is indicative of an efficient use of the adsorbent in dynamic processes, in line with high rate of adsorption. In actual applications, the adsorption columns are regenerated before breakthrough occurs, so one of the main uses of a simulation model is its capacity to predict the breakthrough time (t_b) and the corresponding uptake (q_b). In this work, t_b was defined somewhat arbitrarily as the time corresponding to $C_A/C_0 = 10\%$, although this value may vary according to the specific requirements of each application. In accordance with the generally accepted behavior of a packed bed column, q_b under the smallest flow rate (15 mL min^{-1}) was the closest to q_e, as a result of increased contact time and a shorter mass transfer zone. As seen in Table 8, q_b for TRI-PE-MCM-41 decreased from 1.89 mmol g^{-1} at a flow rate of 15 mL min^{-1} to 1.56 mmol g^{-1} at 50 mL min^{-1}. Considering the particularly short retention time at 50 mL min^{-1}, it can be said that the adsorbent is remarkably efficient as its q_b represents more than 75% of its q_e.

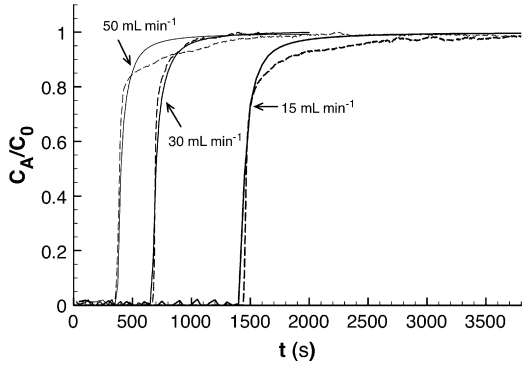

Fig. 7. Experimental (dashed lines) and predicted (solid lines) breakthrough curves of 5% CO_2 balance N_2 on TRI-PE-MCM-41.

Table 8
Experimental and predicted values of t_b and q_b.

F (mL min^{-1})	Experimental[a]		Model	
	t_b (s)	q_b (mmol g^{-1})	t_b (s)	q_b (mmol g^{-1})
15	1524 ± 28	1.89 ± 0.03	1450	1.80
30	714 ± 23	1.77 ± 0.06	675	1.67
50	380 ± 24	1.56 ± 0.09	375	1.54

[a] Average values of three experimental runs.

Because of the excellent behavior of Avrami's kinetic model, it was chosen for the modeling of CO_2 adsorption in a fixed bed column. The concentration of CO_2 downstream the column predicted by the model is also presented in Fig. 7, where it can be compared with the experimental data. Although not shown, a preliminary study to determine the appropriate size of control volumes and time steps was performed by systematically decreasing their values. It was found that under the conditions used in this study, no significant change was observed when the time steps were of 0.01 s or smaller combined with control volumes of less than 1/20 of the total length of the column. All the simulations presented herein were obtained using these values.

As seen in Table 8, the predicted t_b was in all cases close to the experimental data. It is particularly interesting to notice that the breakthrough curve generated by the model reproduced the asymmetry observed in the experimental curve, with a slower increase of downstream concentration beyond C_A/C_0 of ca. 0.60. These results corroborate the utility of the fixed bed column model used to predict CO_2 adsorption on TRI-PE-MCM-41, reflecting the adequacy and usefulness of the proposed kinetic and equilibrium models. Some differences between the predicted breakthrough curves and the experimental data presented in Fig. 7 were observed when C_A/C_0 approached 1, particularly in the breakthrough curves corresponding to 15 and 50 mL min^{-1}. Indeed, some experimental signals showed a slower than expected approach to saturation. However, this behavior did not occur in all cases, indicating that it is most likely attributable to experimental errors, related to either the accuracy of the instrument and/or to a slightly drifting baseline.

Although a small discrepancy (i.e., less than 10%) was observed between the experimental and predicted values of q_b, as shown in Table 8, the latter were consistently lower, suggesting the occurrence of a systematical error. This error might be a result of the assumptions made to solve the fixed bed model, in addition to those of the kinetic and equilibrium models. Nonetheless, considering all the potential sources of error, the level of accuracy observed is a strong indication that the proposed models provide an acceptable representation of the behavior of CO_2 adsorption in a fixed bed column containing amine-functionalized mesoporous silica.

4. Conclusions

This study presented for the first time a kinetic analysis of CO_2 adsorption on amine-functionalized materials at low adsorbate concentrations and an attempt at modeling the behavior of a fixed bed column. The adsorption kinetics of CO_2 on TRI-PE-MCM-41, an amine-grafted mesoporous adsorbent, was successfully described using Avrami's kinetic model with a reaction kinetic order of 1.4. This was attributed to the ability of Avrami's model to describe complex adsorption mechanisms as a result of its fractional order. This model was capable of describing the uptake of CO_2 in the temperature range of 25–75 °C, with a standard deviation of less than 3.5%. It was also demonstrated that TRI-PE-MCM-41 offers more favorable kinetics than PEI-impregnated pore expanded MCM-41 silica. The kinetic model developed herein, in conjunction with the equilibrium model proposed in a previous work, was applied to describe the adsorption of CO_2 in a fixed bed column. By solving the mass balance equation of a fixed bed adsorption column using computational fluid dynamics, t_b was accurately predicted for different flow rates. Moreover, the shape of the breakthrough curve as predicted by the model was in close agreement with the experimental data. This suggests that computational fluid dynamics can be used to describe CO_2 adsorption on amine-containing materials and that the equilibrium and kinetic models developed for the adsorption of CO_2 on TRI-PE-MCM-41 are adequate.

Acknowledgments

The financial support of the Natural Science and Engineering Research Council of Canada (NSERC) and Canadian Institute of Health Research (CIHR) is acknowledged. R.S.-G. thanks the Government of Ontario for a graduate studies scholarship. A.S. thanks the Federal Government for the Canada Research Chair in *Nanostructured Materials for Catalysis and Separation* (2001–2015).

Appendix A. Supplementary data

Supplementary data associated with this article can be found, in the online version, at doi:10.1016/j.cej.2010.04.042.

References

[1] S. Satyapal, T. Filburn, J. Trela, J. Strange, Performance and properties of a solid amine sorbent for carbon dioxide removal in space life support applications, Energy Fuels 15 (2001) 250–255.
[2] H.T. Hwang, A. Harale, P.K.T. Liu, M. Sahimi, T.T. Tsotsis, A membrane-based reactive separation system for CO_2 removal in a life support system, J. Membr. Sci. 315 (2008) 116–124.
[3] S. Cavenati, C.A. Grande, A.E. Rodrigues, Adsorption equilibrium of methane, carbon dioxide, and nitrogen on zeolites 13X at high pressures, J. Chem. Eng. Data 49 (2004) 1095–1101.
[4] J.A. Delgado, M.A. Uguina, J.L. Sotelo, B. Ruiz, M.R. Rosario, Separation of carbon dioxide/methane mixture by adsorption on a basic resin, Adsorption 13 (2007) 373–383.
[5] C. Song, Global challenges and strategies for control, conversion and utilization of CO_2 for sustainable development involving energy, catalysis, adsorption and chemical processing, Catal. Today 115 (2006) 2–32.
[6] H. Yang, Z. Xu, M. Fan, R. Gupta, R.B. Slimane, A.E. Bland, I. Wright, Progress in carbon dioxide separation and capture: a review, J. Environ. Sci. 20 (2008) 14–27.
[7] S. Choi, J.H. Drese, C.W. Jones, Adsorbent materials for carbon dioxide capture from large anthropogenic point sources, ChemSusChem 2 (2009) 796–854.
[8] P.J.E. Harlick, A. Sayari, Applications of pore-expanded mesoporous silica. 5. Triamine grafted material with exceptional CO_2 dynamic and equilibrium adsorption performance, Ind. Eng. Chem. Res. 46 (2007) 446–458.
[9] Y. Belmabkhout, A. Sayari, Effect of pore expansion and amine functionalization of mesoporous silica on CO_2 adsorption over a wide range of conditions, Adsorption 15 (2009) 318–328.
[10] Y. Belmabkhout, R. Serna-Guerrero, A. Sayari, Adsorption of CO_2-containing gas mixtures over amine-bearing pore-expanded MCM-41 silica: application for gas purification, Ind. Eng. Chem. Res. 49 (2010) 359–365.
[11] R. Serna-Guerrero, Y. Belmabkhout, A. Sayari, Further investigations of CO_2 capture using triamine-grafted pore-expanded mesoporous silica, Chem. Eng. J. 158 (2010) 513–519.
[12] R. Serna-Guerrero, Y. Belmabkhout, A. Sayari, A semi-empirical equilibrium model for CO_2 adsorption on amine-functionalized mesoporous silica, Chem. Eng. J. 161 (2010) 173–181.
[13] R. Serna-Guerrero, E. Dána, A. Sayari, New insights into the interactions of CO_2 with amine-functionalized silica, Ind. Eng. Chem. Res. 47 (2008) 9406–9412.
[14] C. Knofel, C. Martin, V. Hornebeq, P.L. Llewellyn, Study of carbon dioxide adsorption on mesoporous aminopropylsilane-functionalized silica and titania

combining microcalorimetry and in situ infrared spectroscopy, J. Phys. Chem. C 113 (2009) 21726–21734.
[15] X. Wang, V. Schwartz, J.C. Clark, X. Ma, S.H. Overbury, X. Xu, C. Song, Infrared study of CO_2 sorption over "molecular basket" sorbent consisting of polyethyleneimine-modified mesoporous molecular sieve, J. Phys. Chem. C 113 (2009) 7260–7268.
[16] W. Rudzinski, T. Panczyk, Kinetics of isothermal adsorption on energetically heterogeneous solid surfaces: a new theoretical description based on the statistical rate theory of interfacial transport, J. Phys. Chem. B 104 (2000) 9149–9162.
[17] S. Azizian, Kinetic models of sorption: a theoretical analysis, J. Colloid Interface Sci. 276 (2004) 47–52.
[18] Y.S. Ho, G. McKay, The kinetics of sorption of basic dyes from aqueous solution by sphagnum moss peat, Can. J. Chem. Eng. 76 (1998) 827–882.
[19] V.J. Inglezakis, S.G. Poulopoulos, Adsorption, Ion Exchange and Catalysis. Design of Operations and Environmental Applications, Elsevier, The Netherlands, 2006.
[20] E.C.N. Lopes, F.S.C. dos Anjos, E.F.S. Vieira, A.R. Cestari, An alternative Avrami equation to evaluate kinetic parameters of the interaction of Hg(II) with thin chitosan membranes, J. Colloid Interface Sci. 263 (2003) 542–547.
[21] A.R. Cestari, E.F.S. Vieira, G.S. Vieira, L.E. Almeida, The removal of anionic dyes from aqueous solutions in the presence of anionic surfactant using aminopropylsilica—a kinetic study, J. Hazard. Mater. B 138 (2006) 133–141.
[22] H.K. Versteeg, W. Malalasekera, An Introduction to Computational Fluid Dynamics. The Finite Volume Method, Prentice Hall, England, 1995.
[23] A. Sayari, Y. Yang, M. Kruk, M. Jaroniec, Expanding the pore size of MCM-41 silicas: use of amines as expanders in direct synthesis and postsynthesis procedures, J. Phys. Chem. B. 103 (1999) 3651–3658.
[24] R. Serna-Guerrero, A. Sayari, Applications of pore-expanded mesoporous silica. 7. Adsorption of volatile organic compounds, Environ. Sci. Technol. 41 (2007) 4761–4766.
[25] X. Xu, C. Song, J.M. Andersen, B.G. Miller, A. Scaroni, Novel polyethylenimine-modified mesoporous molecular sieve MCM-41 type as high-capacity adsorbent for CO_2 capture, Energy Fuels 16 (2002) 1463–1469.
[26] M. Kruk, M. Jaroniec, A. Sayari, Application of large pore MCM-41 molecular sieves to improve pore size analysis using nitrogen adsorption measurements, Langmuir 13 (1997) 6267–6273.
[27] P.J. Barrie, C.K. Lee, L.F. Gladden, Adsorption and desorption kinetics of hydrocarbons in FCC catalysts studied using a tapered element oscillating microbalance (TEOM). Part 2: numerical simulations, Chem. Eng. Sci. 59 (2004) 1139–1151.
[28] C.J. Geankoplis, Transport Processes and Unit Operations, third ed., Prentice-Hall, New Jersey, 1993.
[29] T.C. Drage, A. Arenillas, K.M. Smith, C.E. Snape, Thermal stability of polyethylenimine based carbon dioxide adsorbents and its influence on selection of regeneration strategies, Microporous Mesoporous Mater. 116 (2008) 504–512.
[30] W.J. Son, J.S. Choi, W.S. Ahn, Adsorptive removal of carbon dioxide using polyethyleneimine-loaded mesoporous silica materials, Microporous Mesoporous Mater. 113 (2008) 31–40.
[31] C. Chen, S.T. Yang, W.S. Ahn, R. Ryoo, Amine-impregnated silica monolith with a hierarchical pore structure: enhancement of CO_2 capture capacity, Chem. Commun. 24 (2009) 3627–3629.
[32] X. Ma, X. Wang, C. Song, "Molecular basket" sorbents for separation of CO_2 and H_2S from various gas streams, J. Am. Chem. Soc. 131 (2009) 5777–5783.
[33] Y.S. Ho, Review of second-order models for adsorption systems, J. Hazard. Mater. B 136 (2006) 681–689.
[34] R.M.A. Roque-Malherbe, Adsorption and Diffusion in Nanoporous Materials, CRC Press, Florida, 2007.
[35] V.J. Inglezakis, S.G. Poulopoulos, Adsorption, Ion Exchange and Catalysis: Design of Operations and Environmental Applications, Elsevier, Amsterdam, 2006.
[36] P. Li, H. Tezel, Equilibrium and kinetic analysis of CO_2–N_2 adsorption separation by concentration pulse chromatography, J. Colloid Interface Sci. 313 (2007) 12–17.
[37] B. Royer, N.F. Cardoso, E.C. Lima, J.C.P. Vaghetti, N.M. Simon, T. Calvete, R. Cataluña Veses, Applications of Brazilian pine-fruit shell in natural and carbonized forms as adsorbents to removal of methylene blue from aqueous solutions—kinetic and equilibrium study, J. Hazard. Mater. 164 (2009) 1213–1222.
[38] M.K. Aroua, W.M.A.W. Daud, C.Y. Yin, D. Adinata, Adsorption capacities of carbon dioxide, oxygen, nitrogen and methane on carbon molecular basket derived from polyethyleneimine impregnation on microporous palm shell activated carbon, Sep. Purif. Technol. 62 (2008) 609–613.
[39] M.G. Plaza, C. Pevida, B. Arias, M.D. Casal, C.F. Martin, J. Fermoso, F. Rubiera, J.J. Pis, Different approaches for the development of low-cost CO_2 adsorbents, J. Environ. Eng. 135 (2009) 426–432.